Fibre distribution and orientation of macro-synthetic polyolefin fibre reinforced concrete elements

M.G. Alberti, A. Enfedaque, J.C. Gálvez *, V. Agrawal

Departamento de Ingeniería Civil: Construcción, E.T.S de Ingenieros de Caminos, Canales y Puertos, Universidad Politécnica de Madrid, C/Profesor Aranguren, s/n, 28040 Madrid, Spain

HIGHLIGHTS

- Fibres in PFRC-SCC specimens had better orientation factor poured from the side.
- PFRC-SCC positioning maps showed that there is not a constant flux along the mould.
- The fibre distribution in the VCC specimens was more uniform than in the SCC ones.
- In the vertical elements the coefficient of orientation was stable and around 0.60.
- The flux of SCC in the horizontal element raised the orientation factor.

ARTICLE INFO

ABSTRACT

Fracture behaviour of polyolefin fibre reinforced concrete (PFRC) has proved to be suitable for structural design in construction elements. As in other fibre reinforced materials, the tensile behaviour is strongly affected by the positioning of the fibres. Previous research has assessed this influence by means of fracture tests, showing reliable results. These were obtained by changing the most influencing parameters: the fibre length, the pouring and compaction methods, the concrete type and specimen sizes. However, the influence of these factors in fracture results is merely limited to the fracture surfaces, while the positioning of the fibres in the rest of the piece may be a key factor for design in structural elements. Furthermore, examination of the orientation factor within the whole piece provides relevant information about the behaviour of the fibres during the pouring processes. It may also allow preparation of future models to predict the final positioning of the fibres. This paper examines the positioning and orientation of the fibres in elements which provided fracture results previously reported in the literature. In addition to counting the fibres located in the fracture surfaces, the specimens were divided in portions. The fibre-positioning maps obtained provide sound and useful conclusions that may be considered in future design of PFRC elements. The data gathered showed how the orientation-factor varied with the flux and vibration, absence of any tendency to float and the noticeable influence of the pouring point in fibre distribution. It also showed that this type of fibre is suitable for structural-size elements, improving the orientation factor for longer distances when using self-compacting concrete.

© 2016 Elsevier Ltd. All rights reserved.

1. Introduction

The composite material formed by concrete and fibres is commonly termed fibre reinforced concrete (FRC). The properties provided by the fibres have enhanced one of the major drawbacks of concrete as a building material: its reduced tensile strength. Conventionally, the majority of uses of FRC have entailed a combination of steel fibres and concrete [1], forming what has been termed steel fibre reinforced concrete (SFRC). The improvement of the properties of concrete provided by the steel fibres has allowed its use in several applications, such as industrial pavements and tunnels, among others [2–4]. Furthermore, the contribution of the fibres has recently been considered in structural design [5–7] in the substitution of steel-bar reinforcement of concrete. Subsequently, codes and design standards [8–10] have specified mechanical requirements for structural use. Hence, those fibres capable of meeting residual strengths are the so-called structural fibres, and are typically macro-steel fibres with several shapes such as crimped or hooked-ended fibres.

However, the current concern of society as regards the environmental cost of materials, building processes and infrastructure refurbishment and rehabilitation has given rise to life spans of certain structures of up to 100 years. Therefore, the durability of

materials has emerged as a key factor in the selection of building materials in civil construction. In this regard, the deleterious effects that the environment or soil might have on steel fibres, which may be corroded, have awakened an interest in fibres that are chemically stable and incremented the mechanical performance of concrete. As well as being highly corrosive in nature, steel is expensive to purchase, store and handle. In addition to this, the efforts of the plastic industry have allowed production of a new generation of polyolefin-based synthetic macro-fibres that are inert in an alkaline environment and provide concrete with structural capacities to substitute steel reinforcement [11,12]. Polyolefin fibres have good tensile properties, abrasion resistance and excellent resistance to chemical attacks, which when added to their relatively low cost places them as an alternative to steel reinforcing meshes or steel fibres [13]. Polyolefin fibre reinforced concrete (PFRC) has considerable residual tensile strengths [14–18] with lower weights in comparison with steel fibres. Both the scientific community and the construction industry have identified significant advances in the using plastic fibres to reinforce concrete [19]. Mainly due to the lower cost of the material and lack of corrosion when subjected to hazardous environments, the use of this type of fibres has become attractive [20,21]. PFRC entails multiple sustainability benefits. Recent research focussed on end-of-life cycles has shown the reduction of impact compared with the common practice of using steel reinforcing mesh or steel fibres [22]. The lower dosages in terms of weight needed to reach similar strengths reduce the transportation costs and the size of the carbon footprint. Derived from the production methods, significant decreases in carbon emissions compared with the production of steel can also be found in the literature [23]. Plastic fibres can be directly mixed with concrete without clustering problems and with reduced impact to the workability. Even when using ready-mix trucks the loss of fibres is limited compared with steel fibres [24]. In addition, the handling of this type of fibres is safer, involves less weight, and avoids time-consuming operations such as the preparation and placing of the wire mesh. These aspects permit continuous production of concrete setting with a reduction of labour costs to about half of those when using steel [25]. Hence, PFRC has become an appealing solution that has offered additional benefits if the complete life cycle was considered [26].

The increment of the mechanical properties of PFRC, as in other types of FRC, is significantly affected by a variety of factors, such as the constituent materials of the fibres, geometry and surface treatments. On another note, it is evident that fibre dosage influences performance due to the presence of more fibres acting at a certain surface. However, the action of such fibres varies with fibre inclination and the embedded length, as published research dealing with fibre pull-out has shown [27–29]. Therefore, the distribution and orientation of the fibres modifies the structural response because it entails variations of the number of fibres involved, the fibre angle and embedded length. In such a sense, the reliable use of the fibres is directly associated with knowledge about fibre final positioning in the concrete pieces. Some studies have analysed SFRC, both in conventional and self-compacting concrete, the positioning of fibres and their orientation by means of electromagnetic waves, X-ray radiographies, X-ray computed tomography and image-based analysis [30–34]. Such studies conclude that the rheology of concrete might be a key factor in the positioning of fibres and their orientation in the concrete bulk material. Some published research has evaluated the positioning of polyolefin fibres by means of a CT-scan or X-rays in limited portions of PFRC [35].

If one type of fibre is studied and its dosage is maintained at a steady rate, the main factors that influence fibre distribution and orientation are the concrete properties, pouring and compaction methods, and the formworks and mould sizes. This is of high importance due to the extrapolation of properties assumed when

analysing the mechanical performance of any FRC. Moreover, the possible differences in the positioning of the fibres between the structural-size concrete elements and the laboratory specimens might be also influenced by the pouring processes and even by the size of the fibres used. It is possible to use the formwork and the wall effect with the aim of improving the mechanical response [36]. Some other pouring conditions, such as vertical pours have also been considered [37]. In addition, recent research has assessed the variations on fibre positioning in PFRC elements due to the concrete properties, pouring methods, fibres length and specimen size [38]. Focusing in this last issue, some other publications have assessed the distribution of the fibres in structural-size elements such as concrete slabs [39] or beam elements of more than 2 m-long and vertical elements 0.45 m-long [40]. Most of the discussion about the influence of the various factors involved comparison of the fracture results with the orientation factor at the fracture surfaces. In such a sense, at the time of writing there is few published research about the influence of such factors on the fibre positioning within the rest of the concrete piece. This is of significant interest for structural elements in which the critical section may be uncertain and where a decision as regards the setting processes and concrete type used is required. It may also be decisive for the final shapes of the pieces. The possibility of evaluating how the polyolefin fibres are distributed as a consequence of pouring processes, different formworks and compaction procedures may allow future modelling and a more reliable use of PFRC. This is particularly necessary for the structural-size elements that will become closer to reality.

This research offers an assessment of the distribution of the fibres in the pieces previously studied in Refs. [38,40], examining the effect on the final positioning of the polyolefin fibres by varying the concrete properties and setting processes and specimen sizes. The results provide relevant information for future orientation models that may consider use of synthetic macro-fibres. In addition, this study contributes to a better comprehension of the positioning of the fibres and provides notable data and design considerations for the structural use of PFRC. That is to say, this is studied with a systematic analysis of the positioning and orientation of 6 kg/m^3 of polyolefin fibres added with a variety of external differences. The evaluation was carried out in standard-size specimens (150 × 150 × 600 mm^3) of vibrated conventional concrete with 60 mm-long fibres (VCC6-60). In addition, it was assessed in SCC with 60 mm-long fibres poured in standardised moulds from one side (SCC6-60S) and in SCC with 48 mm-long fibres poured in standardised moulds both from one side (SCC6-48S) and from the centre (SCC6-48C). Moreover, elements similar to real applications were evaluated by manufacturing vertical concrete elements of 150 × 450 × 600 mm^3 manufactured with vibrated conventional concrete with 60 mm-long fibres. Lastly, in a long horizontal element manufactured with SCC with an addition of 60 mm-long fibres, similar to a beam, of 2200 × 250 × 150 mm^3 were analysed. The comparison of the elements with sizes similar to those typically found in building and civil structures with the standard specimens permitted evaluation of the use of laboratory specimens to determine the behaviour and distribution of fibres in PFRC. In addition, it could be argued that obtaining the distribution of fibres in such structural-size elements may provide relevant information about the reliability of the use of this type of fibres in structural elements.

2. Experimental programme

2.1. Materials and mix proportioning

The component materials included Portland cement type EN 197-1 [41] CEM I 52.5 R-SR 5 and a mineral admixture of limestone used as a micro-aggregate. This has a specific gravity and Blaine surface of 2700 kg/m^3 and 425 m^2/kg respectively.

The calcium carbonate content of the limestone powder was higher than 98% and less than 0.05% was retained in a 45 μm sieve. A polycarboxylate-based superplasticizer named Sika Viscocrete 5720 with a solid content of 36% and 1090 kg/m³ density was employed. The mixtures were made with siliceous aggregates composed of two types of gravel with a size of 4–8 mm and 4–12 mm and sand of 0–2 mm. The maximum aggregate size was 12.7 mm.

Polyolefin straight fibres with a rough surface and surface treatment were employed with lengths of 60 and 48 mm. Table 1 shows the main characteristics of the types of fibre, their properties and the geometrical pattern of a 60 mm-long fibre. In all concretes 6 kg/m³ of fibres were added.

The proportions used in vibrated conventional concrete (VCC) and SCC are shown in Table 2. The self-compacting formulation where 6 kg/m³ of 48 mm-long fibres were used was named SCC6-48. Similarly, when 6 kg/m³ of 60 mm-long fibres were employed in the self-compacting formulation, the concrete was termed SCC6-60. In addition, the conventional mix with 6 kg/m³ of 60 mm-long fibres added was named VCC6-60. All the fibre reinforced formulations are also shown in Table 2.

The fresh and mechanical properties of all the types of concrete used can be found in Refs. [38,40].

2.2. Concrete production

The mixing procedures followed for all the concretes used have been previously described in the literature. The achieving of the SCC mix proportioning was reported in Ref. [14]. In the case of the VCC mix proportioning, the basis of the design was described in detail in Ref. [17]. This study has used the specimens tested in Refs. [38,40] prepared with the concrete types and other affecting factors mentioned below. Fig. 1 is offered to aid comprehension of the wording.

The influence of fibre length in fracture results was analysed in Ref. [38]. The same dosage of fibres was added to the same SCC formulation. Whereas one formulation was prepared with 48 mm-long fibres (SCC6-48S), the other was manufactured with 60 mm-long ones (SCC6-60S). In both cases, the SCC was poured in the 600 × 150 × 150 mm³ formworks from one of the sides. Furthermore, the effect of the casting procedure on the distribution of fibres was assessed by comparing SCC6-48S with the same formulation poured from the centre of the specimen SCC6-48C. In all the processes mentioned above, the specimens reached compaction due to their own weight.

The differences in the orientation and density of fibres caused by the vibration process when compared with the self-compaction of SCC were also studied. This was performed by manufacturing a vibrated conventional concrete with a 6 kg/m³ dosage of 60 mm-long fibres named VCC6-60. Two 600 × 150 × 150 mm³ specimens were filled, following the standard process described in EN-14651 [42] and RILEM TC 162-TDF [43]. The specimens were later consolidated for 10 s by means of a vibrating table.

Furthermore, and in order to analyse the effect of the flow, the pouring method and size of the specimens, a beam-shaped wooden mould 2200 mm long, 150 mm high and 250 mm deep was prepared. The formwork was filled with SCC6-60 from one of the sides. The total length of the element was chosen with the aim of obtaining four 550 mm-long specimens suitable for flexural tests. Although the fracture behaviour of the specimens is of great interest, examination of the results and discussion are beyond the scope of this paper and have been previously studied [40]. The specimens were numbered from the casting point (L1) towards the end of the mould (L4). In order to neglect the influence of the wall effect on the specimens, a 50 mm thick lateral wall was removed from each side of the beam element.

Finally, one more series of specimens based on VCC6 was manufactured and named UHD. These research series were produced with the aim of determining any possible floating of the fibre, due to its low density, after 30 s of consolidation on a vibrating table. The moulds had the same dimensions as the standard specimens in both length and depth. Nevertheless, the moulds were three times taller than the standardised moulds. Therefore, the dimensions measured 600 mm in length, 450 mm in height and 150 mm in depth. After 24 h in the laboratory, the concrete was unmoulded and divided into three prismatic specimens of 600 × 150 × 150 mm³. The upper, central, and bottom ones were named, respectively, U, H and D. Similarly to the above mentioned specimens L1–L4, the behaviour of the specimens U, H and D is beyond the scope of this paper and has been discussed in the aforementioned references. In Fig. 1 a summary of the elements analysed in this paper is offered.

3. The fibre distribution and orientation factor

With the aim of analysing fibre orientation, it was considered that if rigid and straight fibres were uniformly distributed and perpendicular to the crack, the theoretical number of fibres (th) placed in any section of the specimens could be estimated by the expressions (1) and (2). Likewise, if the total length of one single fibre were known, with the same cross-sectional surface, and divided by the length of the beam, the fibres would cross the beam th times. If such an optimum fibre distribution took place, the number of fibres resulting from the counting exercise would be equal to th. When this value is compared with the number of fibres counted in one particular section (n), the denominated orientation factor (θ) commonly used in previous research [18,40,43,44] could be computed by using expression (3). The concept was first proposed by Krenchel in 1975 [45] and Soroushian added such an expression in 1990 [46]. Accordingly, if fibres were perfectly aligned, the number counted would match the theoretical value and, therefore, the ratio θ would be the unity. Consequently, the counting process supplies a value that deals with the orientation of the fibres.

$$V_f = \frac{W_f}{\rho \cdot V} \tag{1}$$

$$th = \frac{A \cdot V_f}{A_f} \tag{2}$$

$$\theta = \frac{n}{th} = n \frac{A_f}{V_f A} \tag{3}$$

In (1)–(3) V_f was the fibre volumetric fraction, W_f the weight of the fibres for a reference volume of 1 m³, ρ the fibre density and V the total volume. In addition, A was the cross section of the specimen and A_f the section of one fibre.

The prediction of the orientation factor θ has been assessed for rigid metallic fibres, obtaining values that range from 0.41 to 0.82 [46,47]. The emerging of polyolefin fibres has led to evaluation of such a factor for non-rigid fibres. There are preliminary results focused on the fracture surfaces of specimens manufactured with SCC reinforced with polyolefin fibres [14,17,38–40] and SCC with a cocktail of steel and polyolefin fibres [18], though many factors under question still remain. One main issue of this theoretical perspective is that it neglects the effect of the fibre length. Although

Table 1
Properties of the polyolefin fibres (supplied by manufacturer).

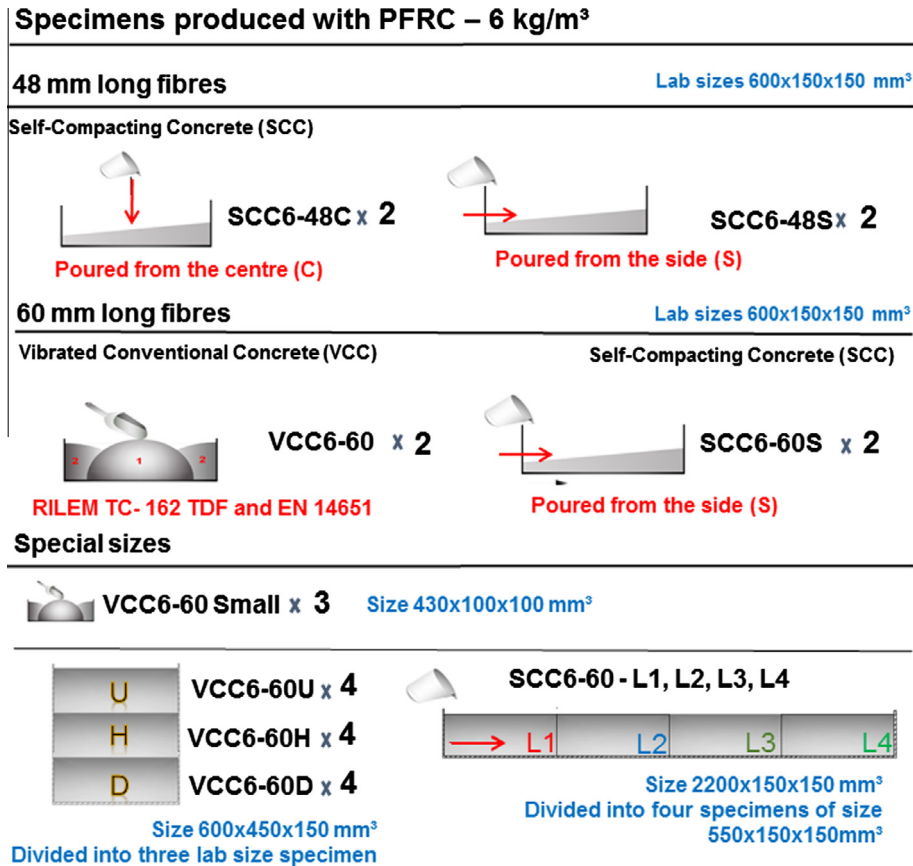|		
Density (g/cm³)	0.91	
Available lengths (mm)	48–60	
Equivalent diameter (mm)	0.92	
Tensile Strength (MPa)	>500	
Modulus of elasticity (GPa)	>10	
Fibers/kg	27.000	

Table 2
Concrete mix proportions (kg/m³) [38].

Concrete type	Cement	Limestone powder	SP (%CEM)	Water	Sand	Grit	Gravel	48 mm-long fibres	60 mm-long fibres
SCC	375	200	1.25%	187.5	918	245	367	–	–
SCC6-48[*]	375	200	1.25%	187.5	918	245	367	6.00	–
SCC6-60	375	200	1.25%	187.5	918	245	367	–	6.00
VCC	375	100	0.75%	187.5	916	300	450	–	–
VCC6-60	375	100	0.75%	187.5	916	300	450	–	6.00

[*] Both SCC6-48S and SCC6-48C were manufactured with the same formulation.

Specimens produced with PFRC – 6 kg/m³

Fig. 1. Concrete elements manufactured in Refs. [38,40].

overlooking this assumption provided reasonably accurate results [46,48], some authors have incorporated more realistic features, such as the wall effect or the use of self-compacting concrete [36,49]. It is worth noting that such models offered by Soroushian [46], Dupont and Vandewalle [48] or the adaptations made from Laranjeira [36] were verified and focus only for the use of steel fibres.

4. Cut surfaces: an orientation factor affected by frameworks and concrete type

Analysis of the positioning of the fibres in concrete has been performed in recent times [50,51]. Most of the published research has examined fibres made from steel. The positioning of the such fibres has been studied by means of a wide variety of methods, such as visual inspection even in full-scale beams [7], electromagnetic methods, X-ray radiography and CT-scan [52,53], among others. However, some of those methods are based on the magnetic properties of the materials and, consequently, may not be applied when the fibres added are polymeric-based materials.

Some published research has evaluated the positioning of polyolefin fibres by means of a CT-scan or X-rays [35,39]. However, such studies have been performed by examining limited portions of PFRC with only one type of concrete in each study used. Due to the high cost of performing a CT-scan inspection of all the specimens tested in this study, one method that incurred lower costs and provided optimum results option was that chosen.

After performing the fracture tests and analysis of the fracture surfaces carried out in previous studies [38,40] were analysed, the resultant half of the specimens was divided into five portions, as Fig. 2 shows. The width of the portions was 60 mm in all the 600 mm-long specimens and 55 mm in the 550 mm-long specimens cut from the beam element. The amount of fibres in each surface was assessed by a counting process. The latter provided the information of the positioning of the fibres in the standardised size specimens. Furthermore, by processing the results of the specimens obtained in the vertical and long elements, the positioning of the fibres in these real-size concrete pieces could be obtained.

In order to compile the data, Table 3 shows the results obtained from the counting process of all the sections. It summarises the positioning of the fibres along the main axis of the specimens and widens the conclusions obtained if only the fracture surfaces were analysed. It should be highlighted that the values obtained along the specimens remained similar to those obtained for the fracture surfaces. The small scatter with coefficients of variation around 15% in most of the cuts is also noticeable. This coefficient was obtained by comparing the theoretical amount of fibres in each section (# th cut) with the average value of the fibres counted in the cut section (#average cut). Therefore, the various values of θ shown in Table 3 were computed by expressions (4)–(6).

$$\theta_{fracture\ surfaces} = \frac{Number\ of\ fibres\ counted\ in\ the\ fracture\ surface}{\#\ th\ in\ the\ fracture\ surface} \tag{4}$$

$$\theta_{specimen} = \frac{Number\ of\ fibres\ counted\ in\ all\ the\ portions\ of\ the\ specimen}{\#\ th\ in\ the\ complete\ specimen} \tag{5}$$

$$\theta_{section} = \frac{Number\ of\ fibres\ counted\ in\ the\ cut\ section}{\#\ th\ in\ the\ cut\ section} \tag{6}$$
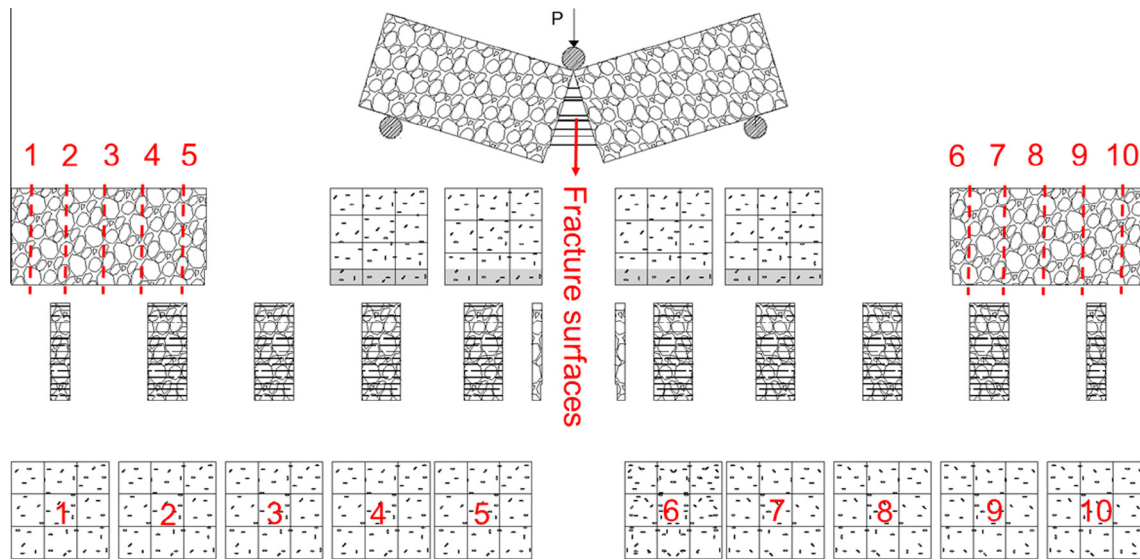
Fig. 2. Portioning of the specimens for the process of fibre counting to assess fibres positioning.

Table 3
Number of fibres on the cut sections, fracture surfaces and the complete specimens.

	Concrete type	Name	Surfaces	Fibre length	# th section	# average cut	c.v.	# th specimen	# average specimen	$\theta_{fracture\ surfaces}$	$\theta_{section}$	$\theta_{specimen}$
Lab-size specimens	VCC6-60	FC6-60	20	60	223	131	0.14	2232	1314	0.57	0.59	0.59
	SCC6-60S	SCC6-60	20	60	223	115	0.17	2232	1146	0.50	0.51	0.51
	SCC6-48C	SCC48	20	48	223	145	0.12	2790	1450	0.64	0.65	0.52
	SCC6-48S	SCC48	20	48	223	164	0.16	2790	1635	0.65	0.73	0.59
Vertical elements	VCC6-60U	U	40	60	223	133	0.13	2232	1329	0.58	0.60	0.60
	VCC6-60H	H	40	60	223	131	0.16	2232	1314	0.51	0.59	0.59
	VCC6-60D	D	40	60	223	143	0.14	2232	1428	0.65	0.64	0.64
	VCC6-60	Vertical elements	120	60	223	136	0.15	6695	4072	0.58	0.61	0.61
Long element	SCC6-60L1	L1	10	60	223	119	0.28	2046	1190	0.54	0.53	0.58
	SCC6-60L2	L2	10	60	223	134	0.08	2046	1343	0.61	0.60	0.66
	SCC6-60L3	L3	10	60	223	143	0.14	2046	1433	0.57	0.64	0.70
	SCC6-60L4	L4	10	60	223	119	0.23	2046	1188	0.60	0.53	0.58
	SCC6	L	40	60	223	129	0.25	8183	5154	0.58	0.58	0.63

After counting the number of fibres in these sections, the orientation factor was obtained in accordance with that previously explained in Eqs. (1)–(3). In addition to the orientation factor of the sections (θ section), an average orientation factor of the specimens was obtained (θ specimen). Table 3 shows that the sections of SCC6-48C or SCC6-48S recorded a value of θ section above the rest of the specimens. This effect might have been caused by the greater amount of fibres added when the 48 mm-long fibre was used. This increment of θ section is caused because the formulation of θ does not take into account the physical characteristics of the fibres, such as fibre length or equivalent diameter, and only considers the theoretical content of fibres. In the rest of the formulations, similar values were obtained, ranging from 0.51 to 0.64. It should also be noted that the highest values were obtained for VCC6-60D specimens and SCC6-60L3. In the case of VCC6-60D, this value might have been due to the influence of the three walls of the mould. However, it should be pointed out that such a value of the orientation factor in the SCC6-60L3 specimens was obtained by removing the sides of the beam element and, therefore, the influence of only one wall of the mould. Consequently, this remarkable value of θ section might be the result of the flux of the SCC.

When comparing the θ section values of SCC6-60S and the SCC6-60L1-L4, the influence of the flux of the SCC can be evaluated. The lower values of θ section identified when SCC6-60S was compared with the SCC6-60L1-L4 values suggest that the limited length of the specimen restrains the flux of concrete and, therefore, the change of orientation in the fibres. This effect can be also assessed in the final portions of the beam elements SCC6-60L1 and SCC6-60L4, where the lowest values of θ section inside the beam element were obtained.

Some details of the experimental procedure performed that should not be overlooked were evaluated by calculating the θ specimen. Such a value was computed by adding the partial counts of all the sections cut and dividing it by the theoretical number of fibres inside the specimen in volume ($th_{specimen}$). That is why for $th_{specimen}$ (as Table 3 shows) there should be more number of fibres, in theory, when shorter fibres where used. Moreover, it should be noted that in those specimens where the width of the portions cut and the length of the fibres coincided with the values of θ section and θ specimen were equal. However, θ section and θ specimen in SCC6-48S and SCC6-48C are different, with θ specimen being lower than θ section. This is because the width of the portions was 60 mm and more fibres were not counted as they did not appear in the surface of the portions and remained inside the portion. When the cuts were made at a distance smaller than the fibre length, some fibres were counted in two surfaces and the value of θ specimen was higher than θ section. This was the case of the specimens obtained from the beam element (from SCC6-60L1 to SCC6-60L4).

In order to obtain an even more detailed evaluation of the positioning of the fibres, all the surfaces processed to obtain Table 3
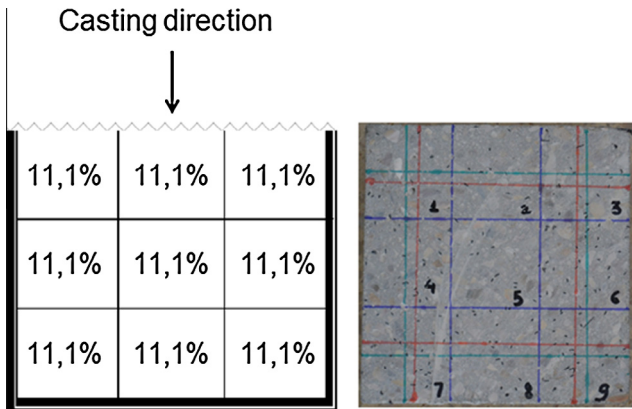
Casting direction

Fig. 3. Uniform theoretical distribution of fibres in a complete sawn surface. The blue lines of the right image divide the concrete section in nine parts.

were divided in nine sectors. A uniform distribution of fibres would lead to a proportional distribution of 11.1% of the fibres placed in each of the nine sectors, as Fig. 3 shows. It should be noted that for this counting and also for the figures, the casting direction is from top to bottom, leaving the free surface in the upper side of the picture or figure.

5. Orientation maps of the concrete elements performed

5.1. Methodology

In order to provide a clearer and easier way to obtain conclusions from the counting process performed, the orientation, and therefore the distribution of fibres have been represented by means of orientation maps. The process followed and explained below can be better understood by observing Fig. 4. In the maps, the values of θ have been represented by means of a colour scale. The process used comprised three steps. The first step was counting the number of fibres placed in each ninth of all the cross sections obtained by means of the aforementioned process. Once this has been done, the number of fibres encountered divided by the theoretical number of fibres that should have appeared in the sector provides the value of θ. As the amount of data is enormous, the average values of θ in the three projections of the specimen were plotted: the side view, top view and front view. Indeed, the bottom-left value of the side view was obtained by averaging the 10 values of θ obtained in the bottom-left sectors of the 10 cross sections analysed. Similarly, the bottom-left value of θ of the top view is the average of the θ values obtained in the nine sectors that

were in the same vertical line. In order to provide conclusions and identify tendencies among the values evaluated, colour maps where the distribution of fibres can be easily distinguished were prepared. For instance, if the area evaluated had no fibres then the value of θ would be zero and the colour of the sector blue. On the contrary, if the amount of fibres counted were equal to the theoretical number of fibres, the value of θ would be one and the colour of the sector red. However, in most cases the colours of the maps range from green to yellow with some reddish areas where the number of fibres is higher.

The especially meticulous manufacturing processes, of key importance in previous studies, in addition to the accuracy provided by the equipment and measuring devices that permitted the reduction of the scatter, should be noted. In the case of the counting procedures, several meticulous counts were made and checked by both calculation and re-counting of the pieces. Thus, the degree of scatter was remarkably low in the case of the vertical elements having four specimens as well as on the two laboratory-size specimens. In the case of the long element, given that only one specimen was produced the conclusions obtained might be strengthened with additional results in future campaigns.

5.2. Fibre positioning in PFRC standard-size elements

Fig. 5 shows the average results obtained in the cut surfaces of the specimens made with SCC6-60S. In the top-right part the average orientation factor of the specimens along the main dimension can be seen. One specimen is represented by the blue line and the other one by a red line. The direction of the flux has been sketched in this plot with an arrow. According to the plot, the orientation factor remains quite stable along the beam, although the pouring location was at one the sides of the mould. It is also important to highlight that at the pouring point the lowest values of the orientation factor were registered for the two specimens. In the middle-right picture of Fig. 5, a sketch of the front view of a specimen with the variation of the orientation factor along can be seen. In addition, the data shown in the front view of the specimen is the average of the orientation factor at every point studied, considering the whole depth of the specimen. Similarly, in the top view of the specimen every point of the map has been obtained as the average orientation factor of the total height of the specimen. The cross section shows the average value of the orientation factor across the length of the specimen. The front view, top view, and the top cross section have been prepared by taking as the extreme values of the orientation factor in the colour scale 0 and 1 which enables a direct comparison among all the concretes studied. In addition, the bottom-side view was prepared by considering, at the sides of the scale, the highest and lowest values of the orientation factor
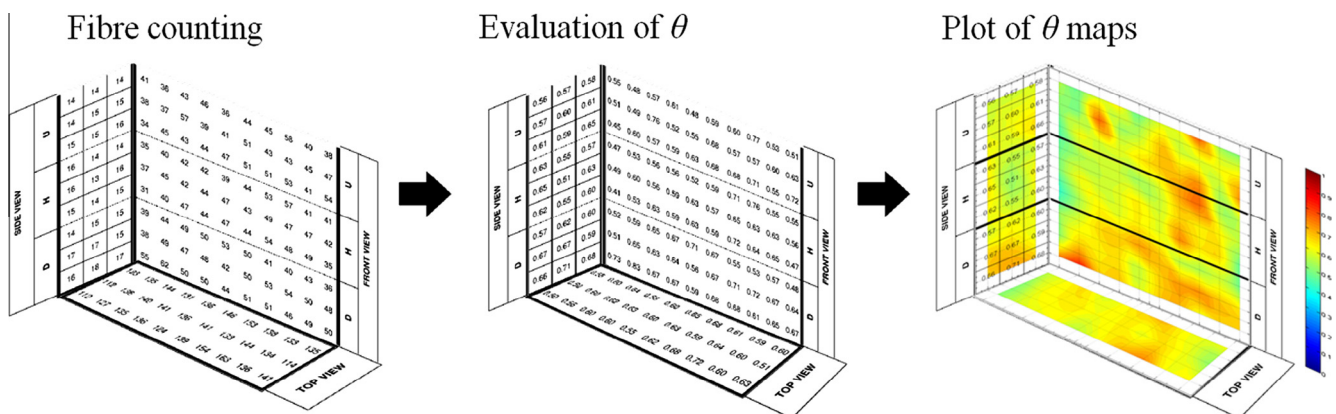

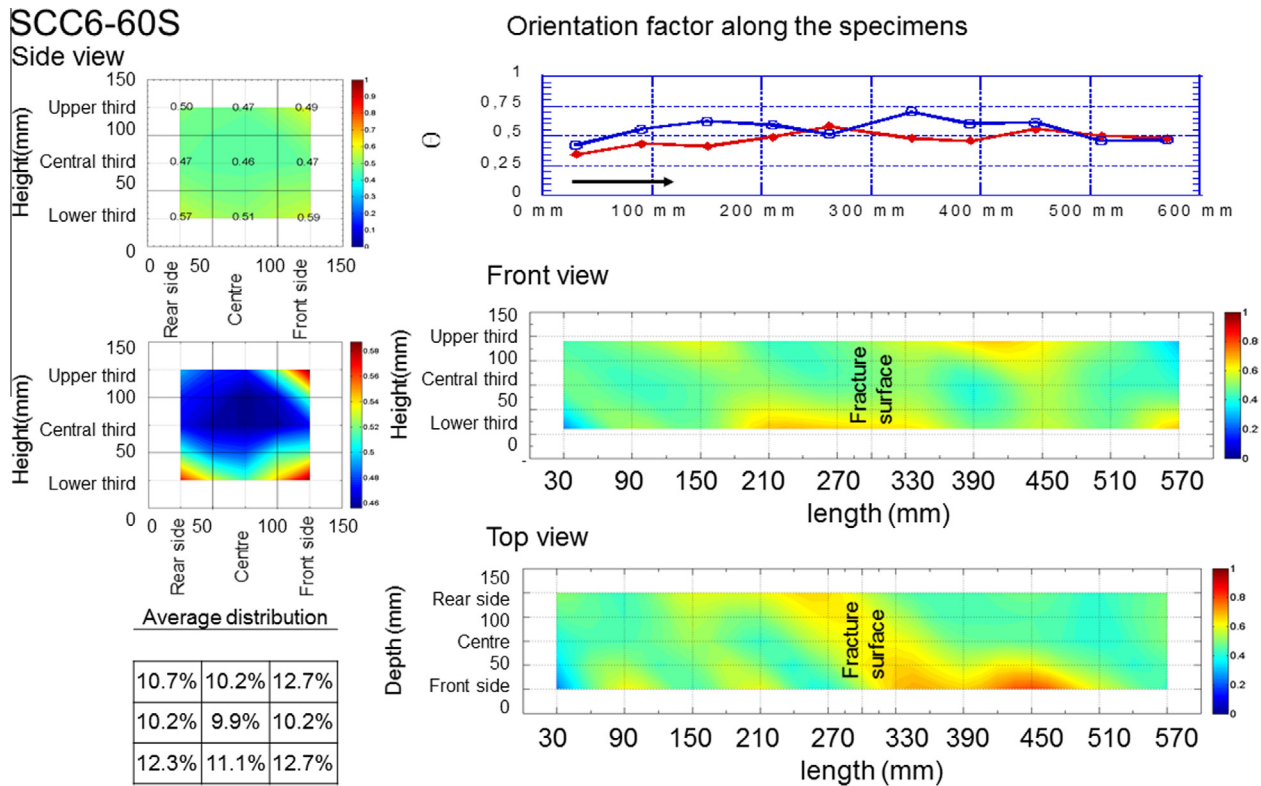**Fig. 4.** Scheme of the methodology used for obtaining the orientation maps.

Fig. 5. Average orientation factor in two SCC6-60S specimens.

within the specimen. This section detects tendencies within the formulation studied. Furthermore, the distribution of fibres in terms of percentage of the total amount of fibres can be seen in the bottom-left part of Fig. 6.

The front view of the average of the orientation factor of SCC6-60S shown in Fig. 6 presents a quasi-homogeneous distribution. The central-bottom part of the specimen concentrated the best orientation of the fibres, while the left and right sides recorded the worst orientation. This is consistent with the limited effect of the flux at the pouring point and the reflux of the concrete towards the centre of the specimen after reaching the wall of the mould.

The top view shows a higher value of the orientation factor in the last part of the specimens. This might be also a consequence of the reflux of concrete. When the cross section is analysed by observing the side view, it may be perceived that it is quite constant, with all the values being between 0.45 and 0.59. However, the highest values confirm the aforementioned wall effect. The distribution of fibres is nearly homogeneous within the section, though it displays higher amounts of fibres in the regions near the walls of the moulds.

Fig. 6 contains the results for VCC6-60 specimens that revealed higher values of the orientation factor in the vibrated concrete with the same dosage of fibres. Similarly to Fig. 5, there are two lines that correspond to the two specimens studied. Scatter along the beam was also small and the orientation factor also increased in the areas close to the corners, probably due to the existence of two physical boundaries. The central sector remained at a below-par percentage value of 10%. The lower third of the cross section also had more fibres counted. In all events, the vibration compaction procedure showed an increment of the orientation factor in the cut surfaces for the 60 mm-long polyolefin fibres as compared with the results obtained for SCC6-60S. Since the upper third of the cross section had the lowest values, no floating effect could be clearly observed in the average distribution.

If Fig. 8 is observed, a remarkable increment of the orientation factor when compared with SCC6-60S may be seen. This has taken place for the two specimens and is quite stable within the length of the specimens. By observing both the front and top view, it is easy to locate a clear concentration of fibres in the whereabouts of the pouring point. The fibres were better oriented in the central sections from the bottom of the specimen almost to the top. It seems that many fibres stayed close to that position and the flux carried some fibres to the sides and flowed to the lower parts of the mould. This effect left more fibres in the centre, near to the fracture surface position and in the lower part of the beam. It should be noted that when there are more fibres in these areas, close to the fracture surfaces, this filling procedure might lead to higher fracture results as shown in [38,40]. It can be also observed that the fibres tend to reach the sides of the moulds quite uniformly in the rest of the beam. When the orientation factor of the cross section is analysed, it can be seen that the orientation factor along the length is clearly influenced by the presence of the walls with the highest values being near to them. The distribution of fibres is consistent with this observation and gathers the highest amounts of fibres in the lowest two thirds of the sections.

When the moulds were filled from one side by using 48 mm-long fibres, as in SCC6-48S, the orientation factor was higher with respect to the values of SCC6-60S or VCC6-60. Moreover, it is somewhat more regular along the specimen, with it being above 0.70 in most of the specimens. This was expected, as explained in the case of SCC6-48C. The orientation of fibres also improved with respect to SCC6-48C. This can be seen by comparing Fig. 7 with Fig. 8. However, it is clear that SCC6-48S had more scatter than SCC6-48C. It is also remarkable that there was a high improvement of the orientation factor in the areas near the pouring point of the concrete, both in the front and top view, as happened in SCC6-48C. The lowest values of orientation factor were obtained for the central sectors, though they were still remarkably high. According to this, the flux enabled
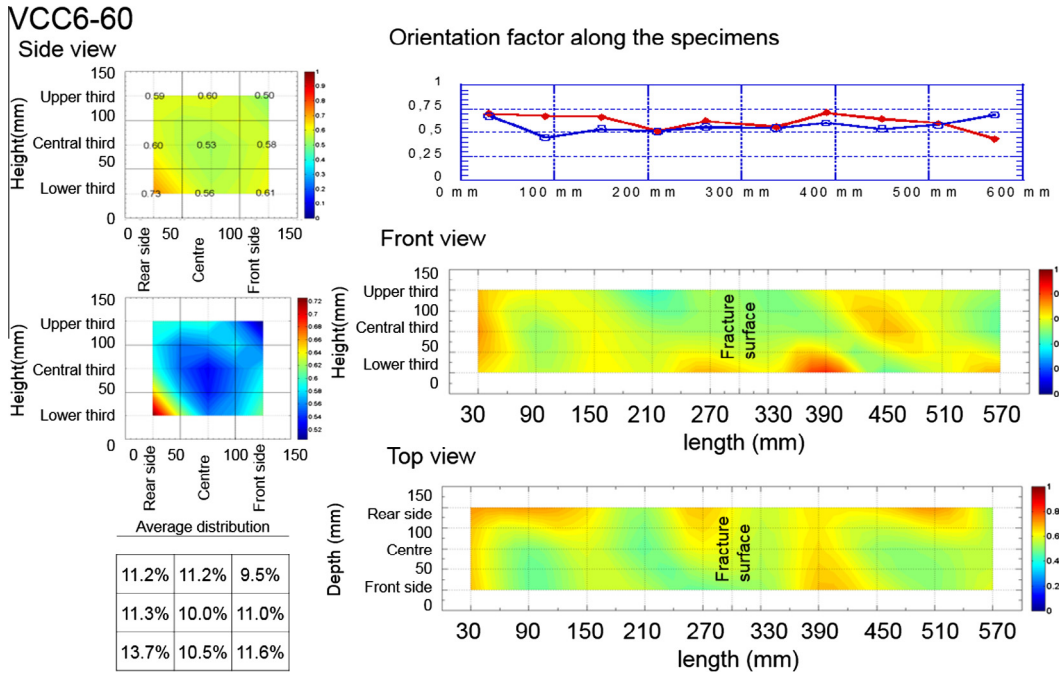
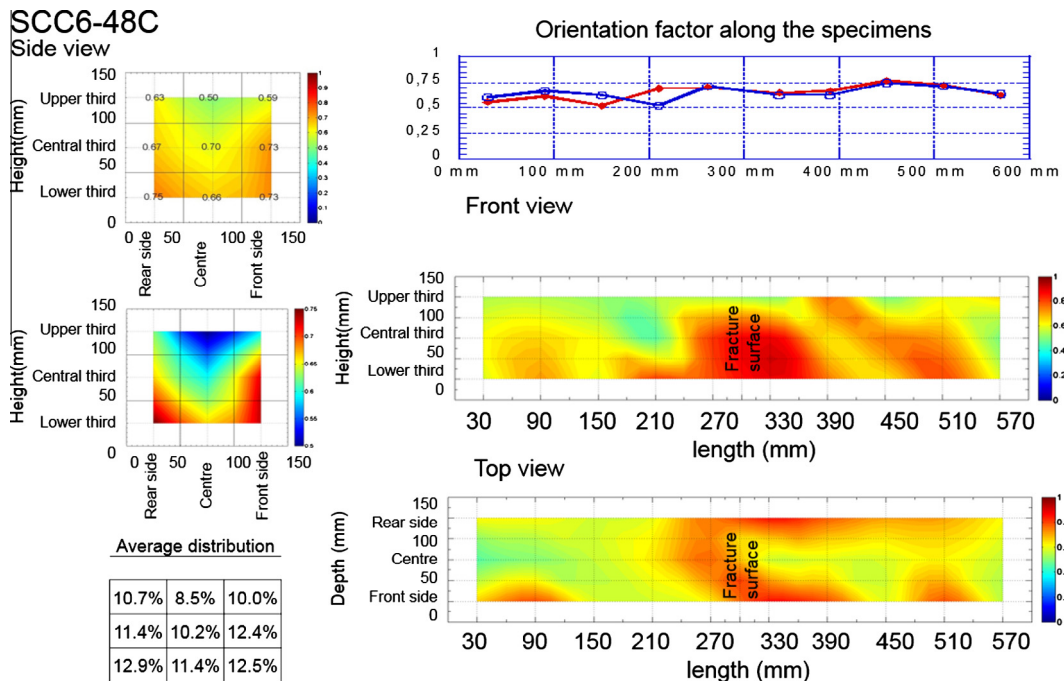**Fig. 6.** Average orientation factor in two VCC6-60 specimens.

Fig. 7. Average orientation factor in two SCC6-48C specimens.

the fibres to reach the end of the beam with high orientation factor values. Only at the very beginning of the beam, could a low value be noticed. This area was probably behind the pouring point of the SCC and was filled in the final moments of the pouring process. The front view placed in Fig. 7 shows the preferential positioning of the fibres in red. The fibres both reached the end of the beam and also became aligned with the direction of the flux. In addition, the improved pref-

erential orientation due to the walls of the mould can be observed in the bottom of the front view and the sides of the top view.

5.3. Fibre positioning in PFRC structural-like elements

Fig. 9 shows the orientation factor of the average of the four specimens of the same relative position. The scatter was small
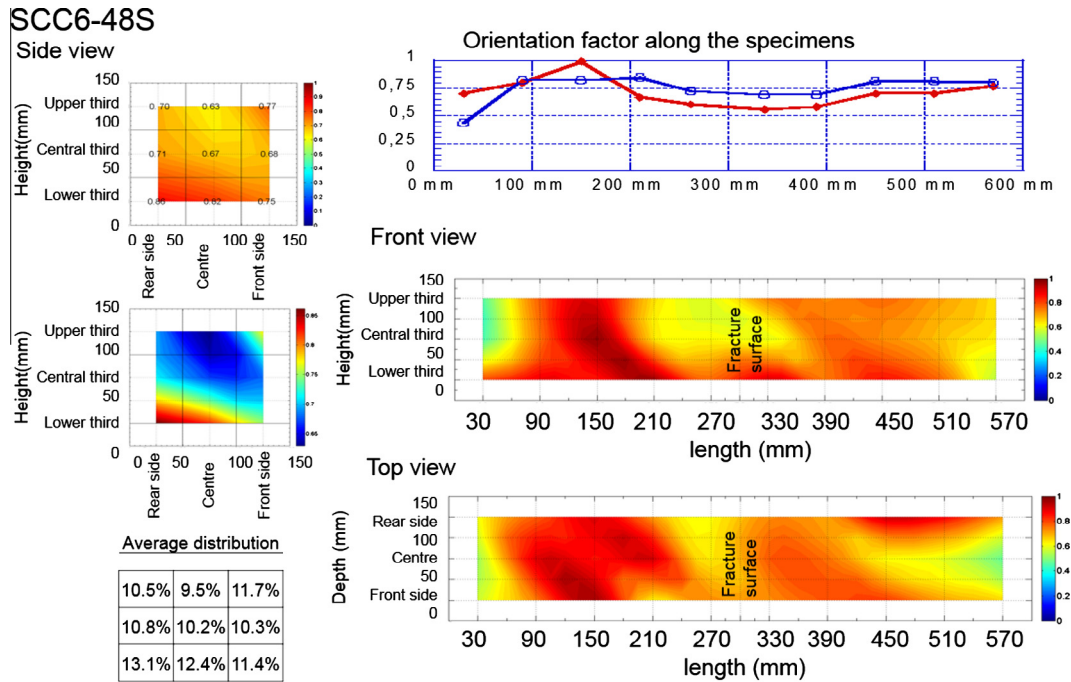
Fig. 8. Average orientation factor in two SCC6-48S specimens.
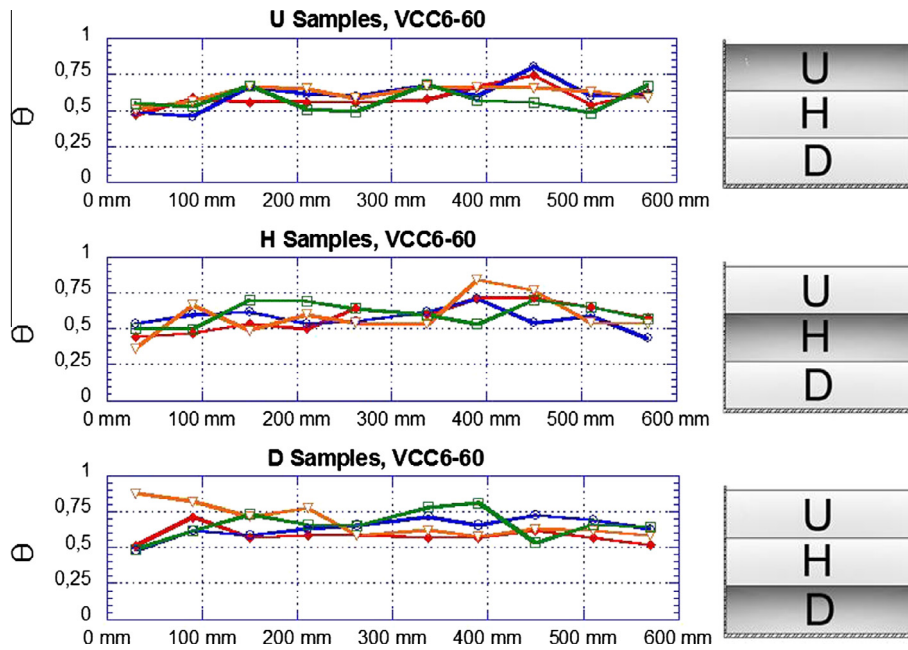

Fig. 9. Orientation factor along the four beams: (a) U specimens; (b) H specimens; (c) D specimens.

among them (U, H and D). In addition, there were no changes in tendency in the positioning of the fibres in the length of the specimens of this vertical element along their main dimension, as can be seen by comparing Figs. 9 and 6. Moreover, in Fig. 9 it can be seen how the values of Θ in the D specimens were slightly higher than those found in the standardised specimens, as well as in the H and U specimens.

In order to assess the possible floating of the fibres caused by the consolidation process within the vertical elements, the orientation factor in the three specimens obtained by cutting each vertical element was evaluated. These results are included in Fig. 10. As can be seen in the figure there were only slight differences in the ori-

entation factor values within the same concrete element, maintaining the θ values obtained in the same range than those obtained in the standard specimens. Although it seems that there has been no displacement of the fibres towards the free surface, a further and deeper analysis was performed to confirm this tendency.

The variation of the orientation factor in height in the four vertical elements manufactured can be seen in Fig. 11. Each point of each vertical element is the average orientation factor of the element for that height, according to Eqs. (1)–(3). Fig. 11 shows, by a black and dashed line, the average value, around 0.6, which is similar to those obtained in SCC with steel fibres. In addition, the
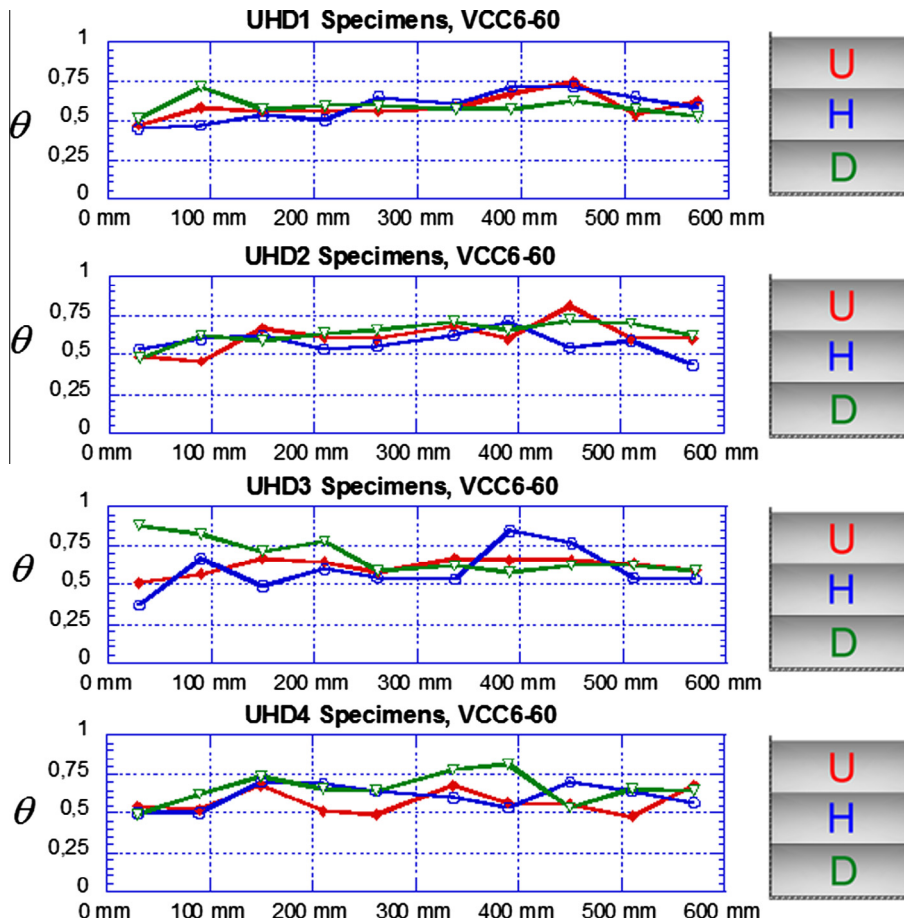
Fig. 10. Evolution of the orientation factor in height in the three specimens of the four vertical elements.
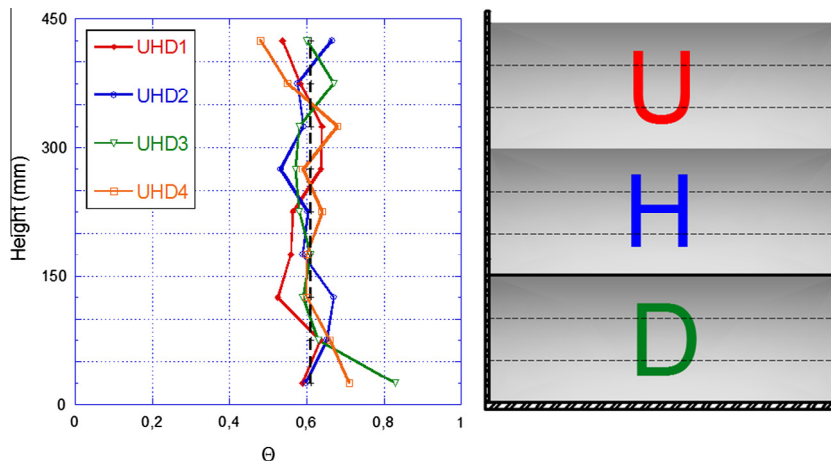

Fig. 11. Average value of the orientation factor in height for the four vertical elements.

orientation factor is quite stable within the height of the concrete element and, consequently, the floating effect of the fibres can be discarded. It is also remarkable that near the bottom of the mould all the values of the orientation factor are close or above the average.

Fig. 12 offers a panoramic view of the distribution of fibres and the variation of the orientation factor in the vertical elements. Similarly to Figs. 5–8, Fig. 12 shows the average values of the orientation factor processed in the four concrete elements in top and front view. Furthermore, it also shows the orientation factor at its cross

section in both relative and absolute scale. In addition, the distribution of fibres within the three specimens obtained can be seen in the right part. The top view shows that the orientation factor of the vertical element has been quite uniform along the main direction of the element. There are only slight changes at both extremes of the element and in one zone near to 450 mm. The front view of the vertical element is of remarkable interest, given that it determines if there is any floatation of the fibres. According to this, it is clear that no vertical displacement of the fibres has occurred. There are greater concentrations of fibres in the lower part of the

tall element and in the upper half of the element. If any floatation had taken place, the distribution of fibres would be higher as the height increases (it was noted that this phenomenon did not happen). This tendency can be more distinguishable in the cross section where the distribution of the orientation factor in the vertical element clearly displays a higher concentration of fibres, and therefore a higher orientation factor, in the lower half of the bottom specimens cut from the complete vertical element. Above

this zone there is a more uniform distribution with subtle increments in the proximity of the walls of the mould.

A similar analysis was performed in the specimens obtained from the long-horizontal element. However, it should be noted that as the sides of the beam element were removed, there was no influence of the lateral walls of the mould on the distribution of fibres. If the orientation factor along the beam element is evaluated, as Fig. 13 shows, it is clear that at the beginning and at the
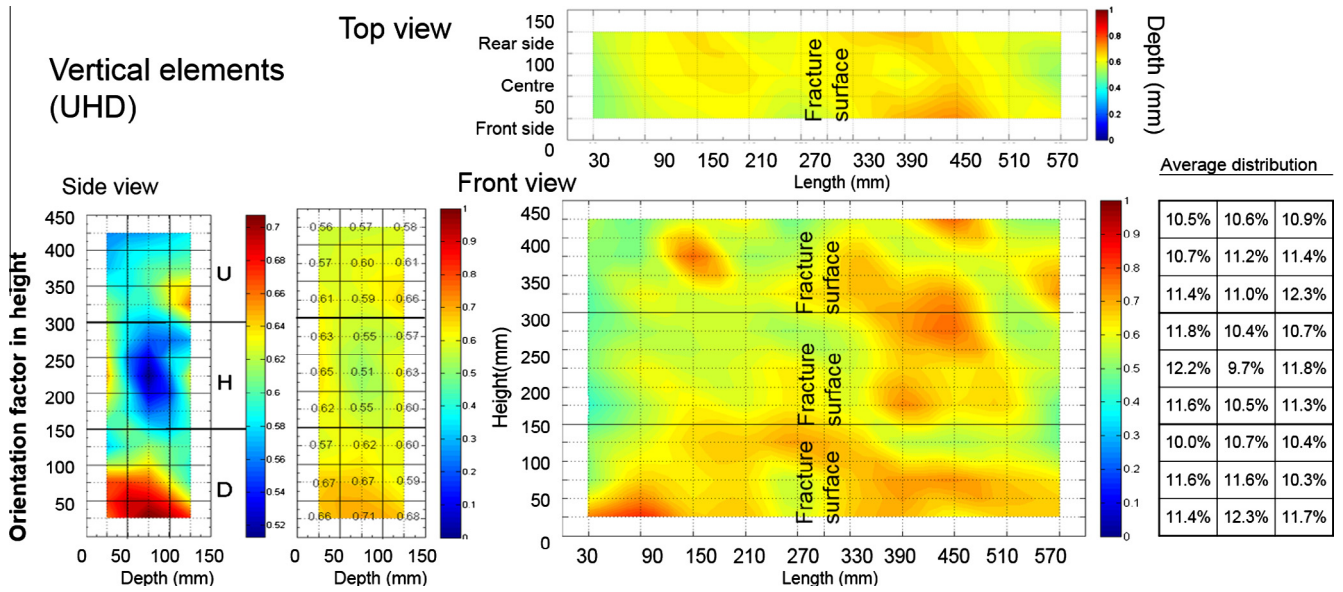

Fig. 12. Average orientation factor in four VCC6-60 vertical elements.
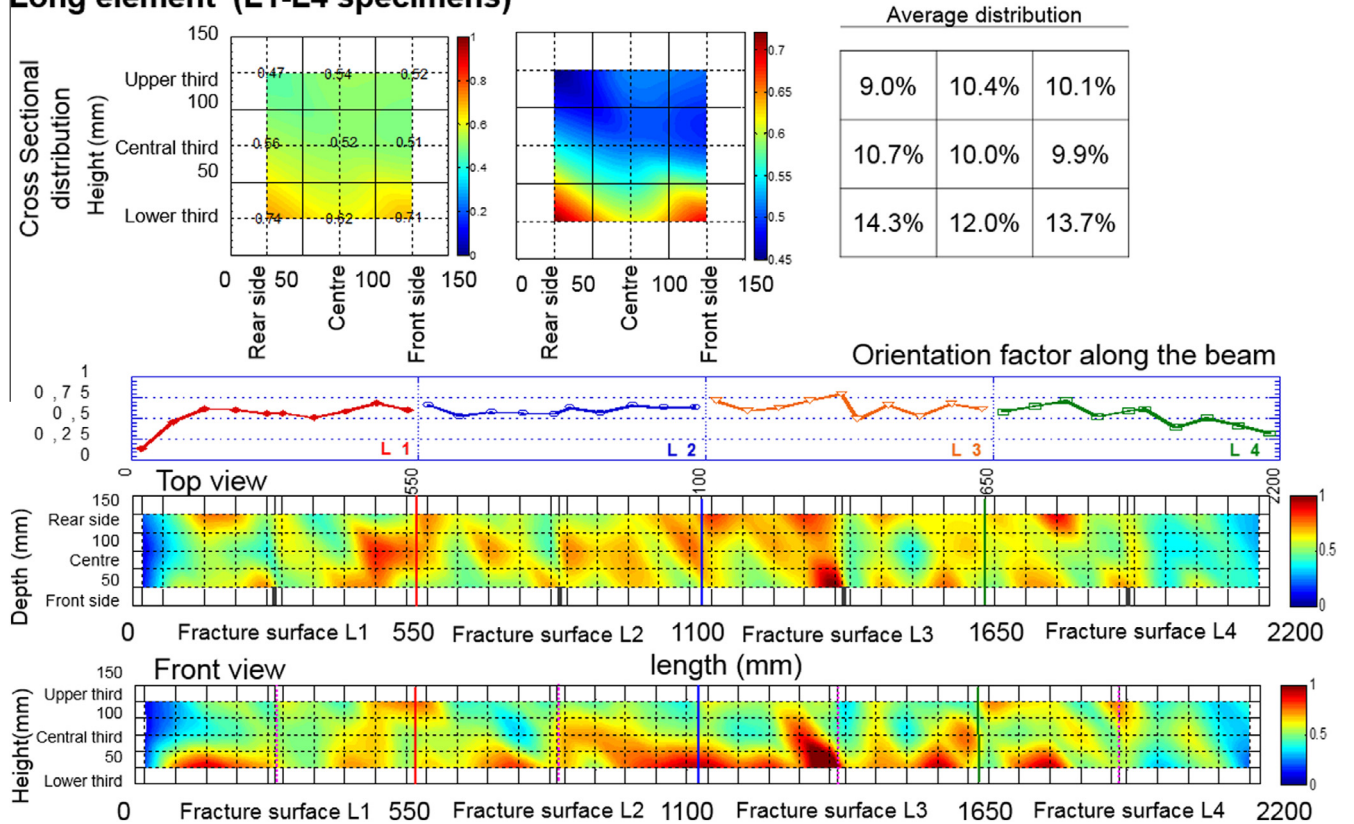

Fig. 13. Summary of the orientation factor in the SCC6-60 Long element.

end of the element the orientation of the fibres is worse than in the rest. This effect could be attributed to the reflux of the concrete when reaching the end of the mould and to the absence of flux in the proximity of the pouring point. Apart from these two areas, the orientation factor is quite stable and in most cases close to 0.6 which is similar to the experimental values obtained for SCC with a the addition of steel fibres [12]. Furthermore, it is important to highlight that the positioning of the fibres within the element was only influenced by the bottom wall of the mould. It should be emphasised that the central beams reached improved orientation factors even with only one wall at the bottom. The improvements achieved began at the first quarter of L1 and ended at the last quarter of L4, which involves around two meters. Therefore, once the flux developed, it helped the fibre to become aligned with it for such a notable distance and reached orientation values above 0.65.

If the cross section shown in Fig. 13 is analysed, it is noticeable that it has more fibres in the lower third. It can be seen that the orientation factor in the lower third of the section reaches values of up to 0.74. This is a clear sign of the preferential orientation that the flux develops in the concrete element. In addition, in the rest of the element it seems that the orientation of the fibres is quite homogeneous. Moreover, there are two aspects that should not be overlooked: the orientation factor of these areas being slightly superior to 0.5 (that predicted for isotropic areas); and the areas near the free surface of the element not showing an increment with respect to the isotropic areas [48].

The top view of the orientation factor shows a remarkably homogeneous distribution of fibres at the same depth, although there were variations along the length. However, it can be seen how the greater values of the orientation factor gather in the central third of the concrete element. Conversely, in the front view it can be clearly observed that the fibre distribution in height was not uniform and that there was a higher value of the orientation factor in the lower surface of the end of L2 and in the middle of L3. In addition, it should be mentioned that the influence of the bottom wall of the mould was clearly noticeable in many parts of the beam if the front view is considered. This tendency confirmed the results obtained from the analysis of the cross section of the beam where the greatest values of the orientation factor were located in the lower third, with the lowest values being at the upper third. Moreover, if the average distribution of fibres along the beam is considered, it is clear that there is a greater amount of fibres in the lower third than in the middle or upper third of the section.

6. Conclusions

In previous works [38,40], the fracture behaviour and the fracture surface analysis showed that the scatter and the residual strengths with 48 mm-long fibres were improved by pouring the self-compacting concrete from the centre. Having said that, this study performed on the specimens a counting exercise that allowed further conclusions that were somewhat unexpected and not measurable without the counting of the portions. It should be noted that even the meticulous procedures allowed a limited degree of scatter, the use of four specimens of each type for the vertical elements, two specimens for the laboratory-size specimens and one specimen for the long element implies that a wider campaign is suggested in order to strengthen some of the following conclusions. Nonetheless, the orientation factor was clearly on average higher in those standard specimens poured from the side. Therefore, the complete concrete piece had, again on average, a better orientation factor when poured from the side even though the fracture results provided the opposite conclusion.

Fracture results also permitted to find that the 48 mm-long fibres showed a better orientation factor when compared with 60 mm-long fibres. The fracture results of both formulations were analogous due to the compensation caused by the higher amount of 48 mm-long fibres pulled out. The orientation factor significantly increased up to 0.73 in the case of 48 mm-long fibres poured from the side. The value of the 60 mm-long fibres poured from the side was confirmed to be 0.51. In all cases, this was measured by using self-compacting concrete.

Continuing with the standard size specimens, the absence of external consolidation energy of self-compacting concrete resulted in a less homogeneous distribution of fibres along the main direction of the standardised specimen when it was poured from one of its sides. In addition, when self-compacting concrete was poured in the centre of the specimens, or when a conventional concrete was used, the distribution of fibres was more uniform.

By analysing the maps of the coefficient of orientation in the specimens manufactured with self-compacting concrete, it was clear that there is not a constant flux along the mould. This effect was explained by the high concentration of fibres in the proximity of the pouring point. Consequently, if the moulds are filled from the centre, the amount of fibres in this area is greater than in the rest of it. Nonetheless, it was concluded that self-compacting concrete would lead to more reliable and comparative results by pouring the mould from the side. In this regard, it is advisable to establish in the testing recommendations that when self-compacting concrete is employed, pouring should be performed from one of the sides of the mould. By manufacturing by such a procedure, the distribution of fibres would represent more reliably the one of the structural elements.

Comparison of the orientation maps of the VCC and the SCC6-60S specimens shows that the consolidation process of the VCC specimens provided a better distribution of the fibres within the specimen. However, it seems that there is a greater influence of the walls in the specimens manufactured with SCC6-60S.

There was no evidence of floatation of the fibres towards the free surface of the mould when a taller mould was filled and vibrated, as was the case of vertical elements. However, the presence of the walls of the mould in the lower parts of such specimens, the D specimens, induced higher concentrations of fibres. It should also be mentioned that the walls of the mould caused an increment of the orientation factor in their surroundings. In the cases of the vertical elements, it was found that the coefficient of orientation was quite stable at around 0.60 both in length and height.

The analysis made in the horizontal element, similar to a beam, showed that when a flux of self-compacting concrete is prepared, the orientation factor rises. Such increment in the lower third of the section was even above the values obtained in previous studies for self-compacting concrete reinforced with steel fibres [36]. This value was considerably high, given that only one wall of the mould affected the orientation of the fibres.

It is worth noting that the conclusions obtained in this study would not have been possible if only the fracture surfaces had been examined. The evaluation of the orientation factor of the complete specimen, based on a counting process, was needed to attain some of the sound conclusions and provide data for future models that may supply predictive tools for macro-synthetic fibres. Such fibres have a behaviour inside concrete that is different from that of rigid steel fibres, due to the polyolefin fibre flexibility and low density.

References

[1] J. Romualdi, J. Mandel, Tensile strength of concrete affected by uniformly distributed and closely spaced short lengths of wire reinforcement, in: ACI Journal Proceedings, 1964.

[2] A. De la Fuente, L. Lin, S. Cavalaro, A. Aguado, Design of FRC tunnel segments considering the ductility requirements of the MC-2010 – Application to the BarcelonaMetro Line 9, in: 2nd FRC International Workshop Fiber Reinforced Concrete: From Design to Structural Applications, 1st ACI-FIB Joint Workshop, Montral, Canada, 2014.

[3] A. Meda, Z. Rinaldi, Steel fibers reinforcement for precast lining in tunnels with different diameters, in: 2nd FRC International Workshop Fiber Reinforced Concrete: from design to Structural Applications, 1st ACI-FIB Joint Workshop, Montreal, Canada, 2014.

[4] S.A. Altoubat, J.R. Roesler, D.A. Lange, K.A. Rieder, Simplified method for concrete pavement design with discrete structural fibers, Constr. Build. Mater. 22 (3) (2008) 384–393.

[5] P. Serna, S. Arango, T. Ribeiro, A.M. Núñez, E. Garcia-Taengua, Structural cast-in-place SFRC: technology, control criteria and recent applications in Spain, Mater. Struct. 42 (9) (2009) 1233–1246.

[6] J.A. López, P. Serna, E. Camacho, H. Coll, J. Navarro-Gregori, First ultra-high-performance fibre-reinforced concrete footbridge in Spain: design and construction, Struct. Eng. Int. 24 (1) (2014) 101–104.

[7] M. Di Prisco, M. Colombo, D. Dozio, Fibre-reinforced concrete in fib Model Code 2010: principles, models and test validation, Struct. Concr. 14 (4) (2013) 342–361.

[8] fib Model Code, Model Code, Paris: Fédération Internationale du Béton fib/International Federation for Structural Concrete, 2010.

[9] CNR-DT 204, Guide for the Design and Construction of Fiber-Reinforced Concrete Structures, Consiglio Nazionale delle Riserche, Roma, 2006.

[10] EHE-08, Spanish Structural Concrete Code, Spanish Minister of Public Works, 2008.

[11] S.C. Ugbolue, Polyolefin Fibres: Industrial and Medical Applications, CRC Press, 2009.

[12] V. Ramakrinshnan, Structural application of polyolefin fiber reinforced concrete, ACI Special Publication 183 (13) (1999) 235–253.

[13] J.E. McIntyre, Synthetic Fibres: Nylon, Polyester, Acrylic, Polyolefin, Elsevier, 2004.

[14] M.G. Alberti, A. Enfedaque, J.C. Gálvez, On the mechanical properties and fracture behavior of polyolefin fiber-reinforced self-compacting concrete, Constr. Build. Mater. 55 (2014) 274–288.

[15] M.G. Alberti, Polyolefin fibre-reinforced concrete: From material behaviour to numerical and design considerations Ph.D. Thesis, Technical University of Madrid, 2015.

[16] P. Pujadas, A. Blanco, S. Cavalaro, A. Aguado, Plastic fibres as the only reinforcement for flat suspended slabs: experimental investigation and numerical simulation, Constr. Build. Mater. 57 (2014) 92–104.

[17] M.G. Alberti, A. Enfedaque, J.C. Gálvez, Comparison between polyolefin fibre reinforced vibrated conventional concrete and self-compacting concrete, Constr. Build. Mater. 85 (15) (2015) 182–194.

[18] M.G. Alberti, A. Enfedaque, J.C. Gálvez, M.F. Cánovas, I.R. Osorio, Polyolefin fiber-reinforced concrete enhanced with steel-hooked fibers in low proportions, Mater. Des. 60 (2014) 57–65.

[19] K. Behfarnia, A. Behravan, Application of high performance polypropylene fibers in concrete lining of water tunnels, Mater. Des. 55 (2014) 274–279.

[20] E.S. Bernard, Durability of cracked fibre reinforced shotcrete, in: Shotcrete: More Engineering Developments: Proceedings of the Second International Conference on Engineering Developments in Shotcrete, Cairns, Queensland, Australia, 2004.

[21] D. Wimpenny, W. Angerer, T. Cooper, S. Bernard, The use of steel and synthetic fibres in concrete under extreme conditions, in: 24th Biennial Conference of the Concrete Institute of Australia, Sydney, Australia, 2009.

[22] S. Yin, R. Tuladhar, F. Shin, M. Combe, T. Collister, N. Sivakugan, Use of macro plastic fibres in concrete: a review, Constr. Build. Mater. 93 (2015) 180–188.

[23] L. Shen, E. Worrell, M.K. Patel, Open-loop recycling: a LCA case study of PET bottle-to-fibre recycling, Resour. Conserv. Recycl. 55 (1) (2010) 34–52.

[24] C. Sorensen, E. Berge, E.B. Nikolaisen, Investigation of fiber distribution in concrete batches discharged from ready-mix truck, Int. J. Concr. Struct. Mater. 8 (4) (2014) 279–287.

[25] T. Ochi, S. Okubo, K. Fukui, Development of recycled PET fiber and its application as concrete-reinforcing fiber, Cement Concr. Compos. 29 (6) (2007) 448–455.

[26] S. Yin, R. Tuladhar, M. Sheehan, M. Combe, T. Collister, A life cycle assessment of recycled polypropylene fibre in concrete footpaths, J. Cleaner Prod. (2015).

[27] V.C. Li, Y. Wang, S. Backer, Effect of inclining angle, bundling and surface treatment on synthetic fibre pull-out from a cement matrix, Composites 21 (2) (1990) 132–140.

[28] P. Robins, S. Austin, P. Jones, Pull-out behaviour of hooked steel fibres, Mater. Struct. 35 (August) (2002) 434–442.

[29] M.G. Alberti, A. Enfedaque, J.C. Gálvez, A. Ferreras, Pull-out behaviour and interface critical parameters of polyolefin fibres embedded in mortar and self-compacting concrete matrixes, Constr. Build. Mater. 112 (2016) 607–622.

[30] H. Al-Mattarneh, Electromagnetic quality control of steel fiber concrete, Constr. Build. Mater. 73 (2014) 350–356.

[31] C. Redon, L. Chermant, J.L. Chermant, M. Coster, Assessment of fibre orientation in reinforced concrete using Fourier image transform, J. Microsc. 191 (1998) 258–265.

[32] T. Ponikiewski, J. Gołaszewski, M. Rudzki, M. Bugdol, Determination of steel fibres distribution in self-compacting concrete beams using X-ray computed tomography, Arch. Civ. Mech. Eng., 2014.

[33] C. Redon, L. Chermant, J.L. Chermant, M. Coster, Automatic image analysis and morphology of fibre reinforced concrete, Cement Concr. Compos. 21 (5) (1999) 403–412.

[34] B. Boulekbache, M. Hamrat, M. Chemrouk, S. Amziane, Flowability of fibre-reinforced concrete and its effect on the mechanical properties of the material, Constr. Build. Mater. 24 (9) (2010) 1664–1671.

[35] J. Kaufmann, K. Frech, P. Schuetz, B. Münch, Rebound and orientation of fibers in wet sprayed concrete applications, Constr. Build. Mater. 49 (2013) 15–22.

[36] F. Laranjeira, A. Aguado, C. Molins, S. Grünewald, J. Walraven, S. Cavalaro, Framework to predict the orientation of fibers in FRC: a novel philosophy, Cem. Concr. Res. 42 (6) (2012) 752–768.

[37] M.C. Torrijos, B.E. Barragán, R.L. Zerbino, Placing conditions, mesostructural characteristics and post-cracking response of fibre reinforced self-compacting concretes, Constr. Build. Mater. 24 (6) (2010) 1078–1085.

[38] M.G. Alberti, A. Enfedaque, J.C. Gálvez, Fracture mechanics of polyolefin fibre reinforced concrete: study of the influence of the concrete properties, casting procedures, the fibre length and specimen size, Eng. Fract. Mech. (2016).

[39] P. Pujadas, A. Blanco, S. Cavalaro, A. de la Fuente, A. Aguado, Fibre distribution in macro-plastic fibre reinforced concrete slab-panels, Constr. Build. Mater. 64 (2014) 496–503.

[40] M.G. Alberti, A. Enfedaque, J.C. Gálvez, V. Agrawal, Reliability of polyolefin fibre reinforced concrete beyond laboratory sizes and construction procedures, Compos. Struct. 140 (15) (2016) 506–524.

[41] EN 197-1, Cement-Part 1: Composition, Specifications and Conformity Criteria for Common Cements, 2012.

[42] EN 14651:2007+A1, Test Method for Metallic Fibre Concrete. Measuring the Flexural Tensile Strength (Limit of Proportionality (LOP), Residual), 2007.

[43] RILEM TC-162-TDF, Bending Test: Final Recommendations, 2002.

[44] L. Martinie, N. Roussel, Simple tools for fiber orientation prediction in industrial practice, Cem. Concr. Res. 41 (10) (2011) 993–1000.

[45] H. Krenchel, Fibre spacing and specific fibre surface, in: Fibre Reinforced Cement and Concrete, The Construction Press, 1975, pp. 69–79.

[46] P. Soroushian, C.D. Lee, Distribution and orientation of fibers in steel fiber reinforced concrete, ACI Mater. J. 87 (5) (1990).

[47] S.T. Kang, B.Y. Lee, J.K. Kim, Y.Y. Kim, The effect of fibre distribution characteristics on the flexural strength of steel fibre-reinforced ultra high strength concrete, Constr. Build. Mater. 25 (5) (2011) 2450–2457.

[48] D. Dupont, L. Vandewalle, Distribution of steel fibres in rectangular sections, Cement Concr. Compos. 27 (3) (2005) 391–398.

[49] F. Laranjeira, S. Grünewald, J. Walraven, C. Blom, C. Molins, A. Aguado, Characterization of the orientation profile of steel fiber reinforced concrete, Mater. Struct. 44 (6) (2011) 1093–1111.

[50] P. Stähli, R. Custer, J.G.M. Mier, On flow properties, fibre distribution, fibre orientation and flexural behaviour of FRC, Mater. Struct. 41 (1) (2007) 189–196.

[51] B.I.G. Barr, M.K. Lee, E.J. de Place Hansen, D. Dupont, E. Erdem, S. Schaerlaekens, L. Vandewalle, Round-robin analysis of the RILEM TC 162-TDF beam-bending test: Part 3—Fibre distribution, Mater. Struct. 36 (9) (2003) 631–635.

[52] P.J. Robins, S.A. Austin, P.A. Jones, Spatial distribution of steel fibres in sprayed and cast concrete, Mag. Concr. Res. 55 (3) (2003) 225–235.

[53] K.J. Trainor, B.W. Foust, E.N. Landis, Measurement of energy dissipation mechanisms in fracture of fiber-reinforced ultrahigh-strength cement-based composites, J. Eng. Mech. 139 (7) (2013) 771–779.